JOURNAL OF MAGNETIC RESONANCE, Series B **111,** 300–304 (1996)
ARTICLE NO. 0098

Temporal Dynamics of Hyperpolarized ^{129}Xe Resonances in Living Rats

KUNIYOSHI SAKAI,* ANASTACIA M. BILEK,* EDUARDO OTEIZA,† RONALD L. WALSWORTH,† DILIP BALAMORE,‡ FERENC A. JOLESZ,* AND MITCHELL S. ALBERT*

*Department of Radiology, Brigham and Women's Hospital and Harvard Medical School, 221 Longwood Avenue, Boston, Massachusetts 02115; †Harvard–Smithsonian Center for Astrophysics, Cambridge, Massachusetts; and ‡Department of Engineering/Physics/Technology, Nassau Community College, Garden City, New York

Received April 16, 1996

Recent development of a magnetic-resonance technique using hyperpolarized noble gases (^{3}He and ^{129}Xe) has enabled imaging of the lung gas space (*1, 2*). While the extremely low solubility of ^{3}He in the blood (*3*) precludes its use as a tissue imaging probe, ^{129}Xe is highly lipophilic and soluble in blood and tissue, and thus holds promise for tissue imaging and physiological studies such as white matter perfusion, heretofore not possible. Recently, hyperpolarized ^{129}Xe tissue signals were reported from a live mouse (*4*). It remains unclear, however, what the lifetimes of different hyperpolarized ^{129}Xe tissue resonances will be *in vivo,* and which tissue will yield distinguishable signals. In this paper, we report measurements of the xenon exchange and accumulation in the pulmonary tissue by examination of the wash-in and wash-out dynamics of hyperpolarized ^{129}Xe signals and their lifetimes in living rats. The *in vivo* spectra exhibited four resolved peaks of hyperpolarized ^{129}Xe resonances from gas, blood, and tissue phases (*5, 6*). In addition, imaging of the lung gas space was performed using hyperpolarized ^{129}Xe. These results suggest applications of the hyperpolarized ^{129}Xe MRI technique for ventilation–perfusion studies of the lung.

The novel technique of noble gas hyperpolarization, by collisional spin exchange with optically pumped rubidium vapor, yields up to a hundred thousandfold enhancement in spin polarization and MR detectability (*7–10*). We used natural-abundance xenon (26% ^{129}Xe), which was contained in a 25 cm^3 cylindrical glass cell, at 3 atm, along with N_2 buffer gas and a small quantity of solid Rb. ^{129}Xe was hyperpolarized in the fringe field of a 4.7 T superconducting magnet (Oxford Instruments, Oxford, UK). Circularly polarized 795 nm light from diode laser arrays (Optopower, Tucson, Arizona) was used for optical pumping of the Rb vapor. After 30 min of optical pumping at 90–100°C, the glass cell was rapidly cooled in ice water to remove the Rb vapor by condensation onto the cell walls. The hyperpolarized ^{129}Xe was extracted by connecting a 25 cm^3 glass cell immersed in liquid nitrogen, for cryopumping the ^{129}Xe from the hyperpolarization cell. The frozen ^{129}Xe was then warmed to room temperature, with minimal loss of its hyperpolarization after sublimation. The hyperpolarized ^{129}Xe gas was transferred to a 50 cm^3 glass syringe prior to use.

Sprague–Dawley rats (400–500 g) were anesthetized with intramuscular injections of ketamine (24 mg/kg) and xylazine (6 mg/kg). A 14 gauge Teflon catheter was inserted into the trachea, and silk ligatures were tied around the endotracheal tube. The animal was then placed in a short birdcage detector coil covering only the thorax. The hyperpolarized ^{129}Xe gas was delivered from the syringe to the animal's lungs via a 24 gauge catheter that was inserted coaxially into the 14 gauge catheter. The animal breathed naturally through the open end of the 14 gauge catheter. In each spectroscopy experiment, four 10 cm^3 boluses of hyperpolarized ^{129}Xe were administered at 4–5 s intervals. The use of an open delivery system allowed excess xenon to escape without injuring the animal from a dangerous built-up pressure. Furthermore, the excess xenon gas was expelled outside the pickup coil. All rats showed no discomfort after the xenon delivery, indicating that the xenon ventilation and the method of delivery were well tolerated. The care and use of animals in these experiments were approved by the Harvard Medical School Standing Animal Committee and conformed with the guidelines set forth by the National Institute of Health (*11*).

^{129}Xe spectra were obtained at 55.35 MHz on a 4.7 T Omega spectroscopy/imaging system (Bruker Instruments, Fremont, California). A spectral window of 25.0 kHz covered both gas and tissue ^{129}Xe resonances. The transmitter frequency was set to 160 ppm downfield from the gas resonance. Free-induction decay data were acquired with low flip-angle (26°) rectangular pulses (pulse width, 100 μs) at 1–3 s intervals. The data were baseline corrected, apodized by Gaussian multiplication (50 Hz for Figs. 1 and 2), and Fourier transformed. Hyperpolarization lifetimes were estimated by the method of least squares for single-exponential line fitting for decaying signals, after correcting the signal magnitudes of each spectral peak for the amount of depolarization induced by the RF excitations.

1064-1866/96 $18.00

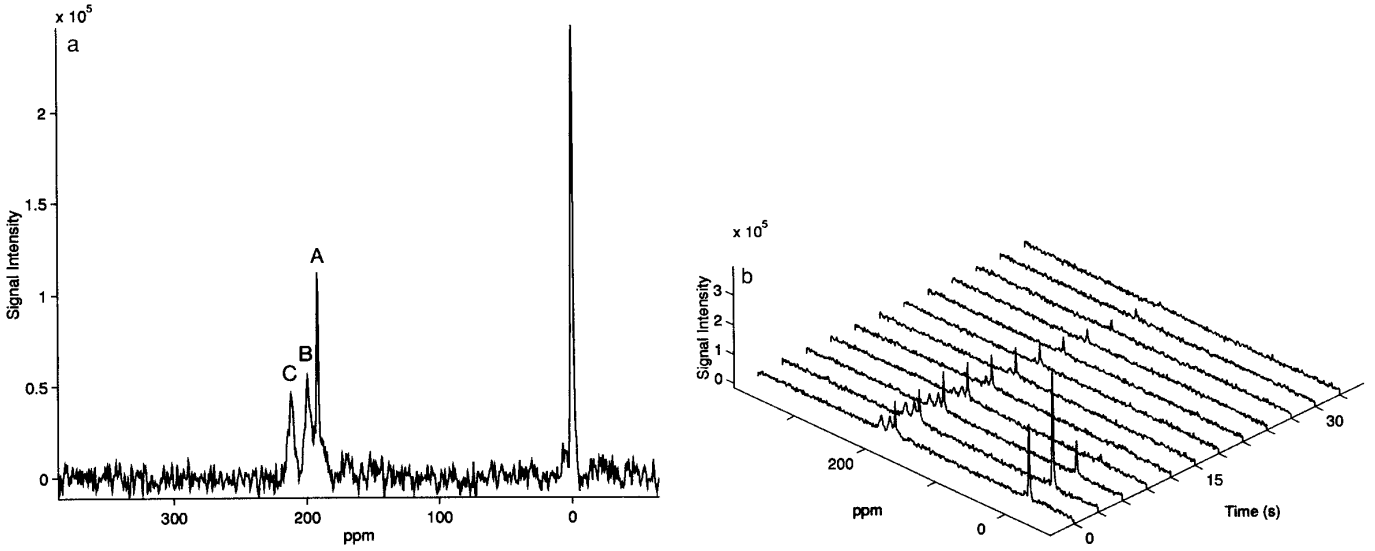

FIG. 1. Hyperpolarized ^{129}Xe resonances and wash-out dynamics in the rat pulmonary system. Data acquisition was started ($t = 0$) at the *last* xenon bolus. (a) Hyperpolarized ^{129}Xe spectrum at $t = 0$. Relative to the largest peak of ^{129}Xe resonance in the lung gas space (0 ppm), three peaks are labeled: peak A at 191 ppm, peak B at 199 ppm, and peak C at 213 ppm. Note a broad companion peak at the base of peak A. (b) Temporal dynamics of hyperpolarized ^{129}Xe resonances. A time series of spectra are shown (one spectrum per 3 s), before correcting for the amount of depolarization induced by the RF excitations. The same phase corrections were applied to all of the Fourier transformed data. Note that peak A at 191 ppm showed the longest lifetime of polarization.

We observed hyperpolarized ^{129}Xe resonances from the pulmonary system of living rats. Figure 1a illustrates the first spectrum obtained in one experiment during the decay and wash-out phase of hyperpolarized ^{129}Xe. The spectrum shows a large lung gas peak at 0 ppm and three distinct peaks at 191 ppm (peak A), 199 ppm (peak B), and 213 ppm (peak C). The chemical shifts of the three peaks, obtained from four separate experiments with different rats, are shown in Table 1.

Figure 1b displays a stacked plot of the hyperpolarized ^{129}Xe spectra during the time course of the experiment and reveals the decay of the ^{129}Xe resonances *in vivo.* Data acquisition was commenced during delivery of the *last* xenon bolus ($t = 0$) and spectra were collected every 3 seconds (TR = 3 s). The lung gas peak, peak B, and peak C reach maxima within 3 s and then decay, whereas peak A reaches a maximum at 6 s. The time course of the gas ^{129}Xe signal reflects not only its own T_1 decay, but also gas exchange with the external air and transport of xenon from the lung space to the pulmonary capillaries. The polarization lifetime constants of ^{129}Xe signals in the blood and tissue are designated here as T_1^* (apparent T_1) and reflect not only T_1 decay, but also wash-out processes including the multicompartmental circulation of xenon in the blood and tissue. Measurements of peak B and peak C yielded T_1^* values of 26.0 ± 2.8 and 11.4 ± 2.2 s, respectively (Table 1). On the other hand, peak A decayed much more slowly with a T_1^* of 49.6 ± 13.8 s (Table 1). The correlation coefficients for the line fitting ranged between 0.77 and 0.98.

Further wash-in experiments shown in Fig. 2, in which data acquisition was started ($t = 0$) before the *first* hyperpolarized ^{129}Xe bolus delivery, reveal the temporal dynamics of the individual peaks. The oscillation of the lung gas peak

TABLE 1

Chemical Shifts and Lifetimes (T_1^*) for Individual ^{129}Xe Peaks in Spectra[a]

	Data set	Chemical shift (ppm)	T_1^*(s)
Peak A	1	191.9	30.3
	2	191.4	50.3
	3	191.4	55.8
	4	191.0	62.1
	Mean ± SD	191.4 ± 0.4	49.6 ± 13.8
Peak B	1	199.8	26.2
	2	198.1	28.2
	3	199.4	22.0
	4	198.5	27.6
	Mean ± SD	199.0 ± 0.8	26.0 ± 2.8
Peak C	1	212.2	14.0
	2	214.4	11.8
	3	212.6	8.7
	4	213.1	11.1
	Mean ± SD	213.1 ± 1.0	11.4 ± 2.2

[a] The frequency of the lung gas peak was set to 0 ppm for reference in each of the four separate experiments. Peaks A, B, and C correspond to the peaks shown in Fig. 1a.

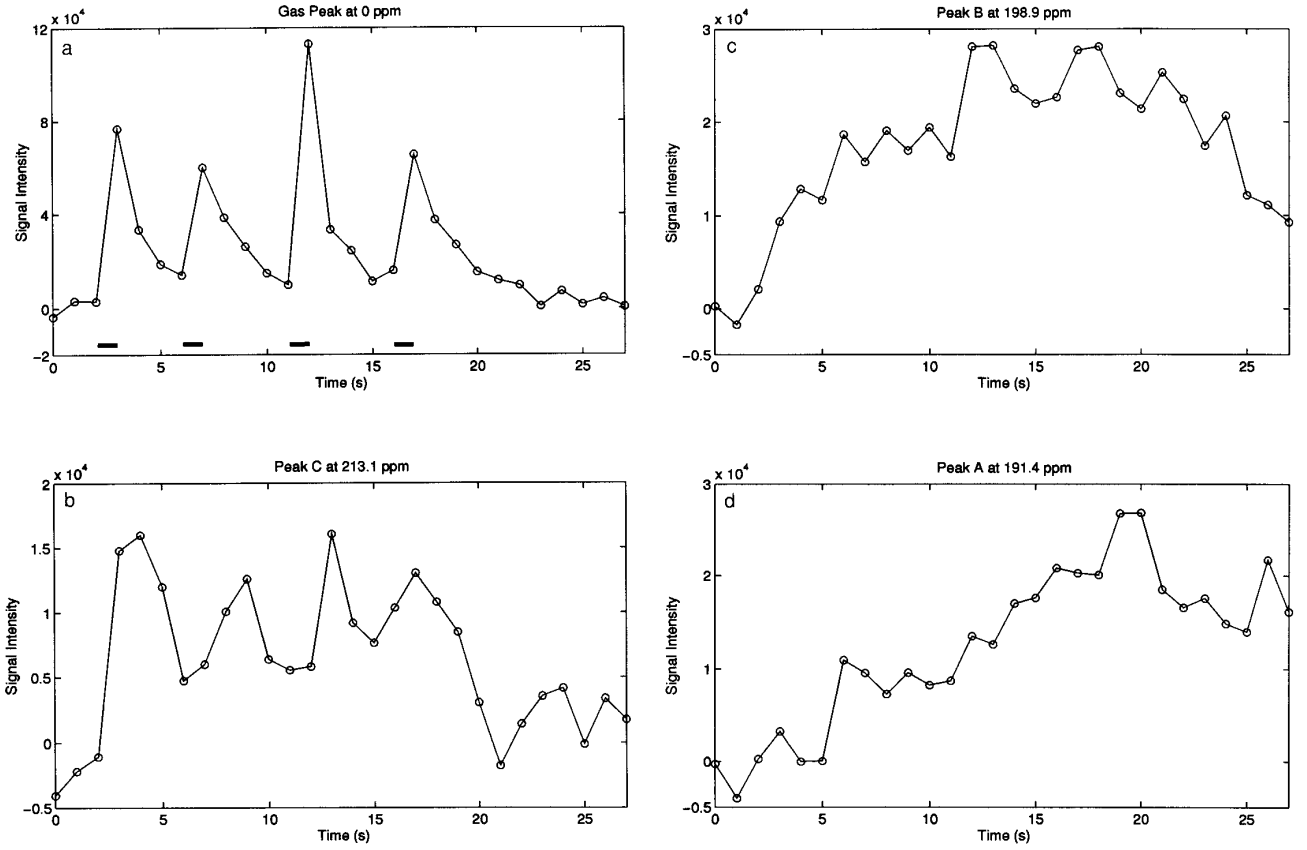

FIG. 2. Wash-in dynamics of individual ^{129}Xe resonances. Data acquisition was started ($t = 0$), 3 s before the *first* xenon bolus. The same phase corrections were applied to all of the Fourier transformed data. For each peak, averaged signal intensities within a 2 ppm window in each spectrum were plotted against time. Noise amplitude mean was $(4.1 \pm 0.2) \times 10^3$, calculating the standard deviation of signal intensity for spectral points where there is no peak in each spectrum. (a) Temporal dynamics of the lung gas peak. The oscillation of this signal is due to the pulsed delivery of ^{129}Xe boluses (thick bars) into the lung. (b) Temporal dynamics of peak C. Note that the oscillation of peak C closely follows that of the lung gas peak with a 1–2 s delay. (c) Temporal dynamics of peak B. Note the different scale of the ordinate. (d) Temporal dynamics of peak A. Note that peak B shows a steady rise followed by the more gradual rise of peak A.

(Fig. 2a) displays the pulsed delivery of ^{129}Xe boluses (thick bars along the abscissa) into the lung. The oscillation of peak C (Fig. 2b) closely follows that of the lung gas peak (Fig. 2a), but with a 1–2 s delay. In contrast, peak B shows a steady rise (Fig. 2c), followed by the more gradual rise of peak A (Fig. 2d). These distinct time courses reflect hyperpolarized ^{129}Xe wash-in processes; the lung gas peak and peak C probably indicate ^{129}Xe exchange processes, whereas peak B and peak A likely reflect ^{129}Xe accumulation processes. These results provide clues for the assignment of the ^{129}Xe resonances.

We suggest a possible assignment of the four distinct peaks in the hyperpolarized ^{129}Xe spectra. The peak at 0 ppm (reference) is clearly from the lung gas, both because it is the largest peak when ^{129}Xe gas is delivered into the lung and because its frequency corresponds to that of ^{129}Xe gas in a glass cell. The assignment of the other three ^{129}Xe peaks is partially based on a comparison with the chemical-shift values from a previous *in vitro* study of thermally polarized ^{129}Xe in the plasma and red blood cell (RBC) components of human venous blood (*12*). In that study, the ^{129}Xe plasma signal was observed at 194 ppm downfield from the gas peak, whereas the ^{129}Xe RBC signal was observed at 216 ppm. Because of their relative chemical shifts, we suggest that peak A at 191 ppm and peak C at 213 ppm correspond to ^{129}Xe in the plasma and RBC components, respectively. The 3 ppm difference between *in vivo* and *in vitro* data is probably a volume susceptibility effect, as the *in vitro* data were obtained from a spherical sample. Thermally polarized ^{129}Xe dissolved in a cylindrical sample of beef fat *in vitro* also exhibits a signal with a 191 ppm chemical shift; we propose that peark A is a superposition of both plasma and adipose tissue signals. Furthermore, the wash-in dynamics of peak C, which closely follows that of the lung gas peak (Figs. 2a, 2b), indicates that ^{129}Xe rapidly exchanges into the RBCs [most probably binding to hemoglobin (*13*)]. The RBCs in alveolar capillaries are separated from the lung gas space by an extremely thin blood–gas barrier of pulmonary tissue (*14*). The rapid appearance of the putative RBC signal (peak

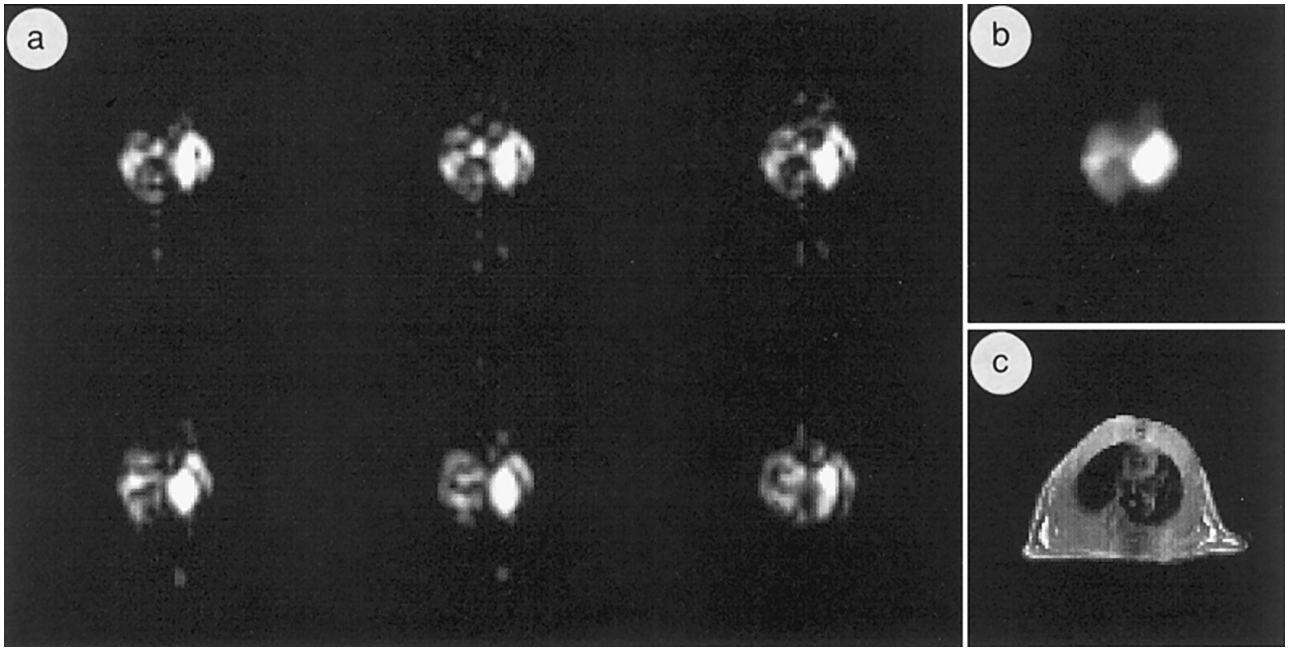

FIG. 3. MR lung images of a living rat. (a) Temporal sequence of consecutive axial images of hyperpolarized ^{129}Xe signals from the lung gas space. The sequence follows from the left to the right side, from the top to the bottom row. Note that the region of the highest ^{129}Xe signal shows lower intensity in later frames. These images were acquired with a FLASH pulse sequence (TR = 21 ms; TE = 10.5 ms; flip angle, 30°; in-plane resolution, 2.3×4.7 mm^2; slice thickness, 15 mm), while xenon gas was delivered in short boluses every 0.5 s. The acquisition time for each image was 1.3 s. (b) The summed image from the six images shown in (a). (c) A corresponding axial ^{1}H image of the same animal. This image was acquired with a spin-echo pulse sequence with T_1 weighting (TR = 500 ms; TE = 18 ms; in-plane resolution, 0.35×0.35 mm^2, slice thickness; 10 mm) on a 1.5 T Signa imaging system (GE Medical Systems, Fremont, California).

C) is consistent with xenon's high affinity for hemoglobin (*13*) and close proximity of the RBCs to the gas space in the alveolar capillaries. The delayed appearance and slow accumulation of peak A (Fig. 2d) may be due to diffusion of ^{129}Xe from the RBCs into the plasma and then into adipose tissue. The plasma pool may include plasma in blood vessels distal to the capillary network of the lung. The longer rise time for peak A is consistent with its long T_1^*.

Because peak B appears simultaneously with peak C (Figs. 2b, 2c), we suggest that peak B corresponds to ^{129}Xe in pulmonary tissue. Pulmonary tissue includes the layer of surfactant, alveolar epithelium, interstitium, and capillary endothelium (*14*). The pulmonary tissue adjacent to the capillaries is in contact with the lung gas, which would allow for an early onset of the tissue signal (peak B). The picture that emerges from our peak assignment is that inhaled hyperpolarized ^{129}Xe first washes into the RBCs in transit in the alveolar capillaries and into pulmonary tissue in contact with the gas. The ^{129}Xe in the RBCs then gradually washes out into the plasma and adipose tissue, giving rise to peak A.

Because we have used a periodic ^{129}Xe bolus delivery procedure in the wash-in experiments, the concentration of hyperpolarized ^{129}Xe, in the lung gas space, has a periodicity (Fig. 2a). Taking account of the T_1^* of 11.4 s for the putative RBC signal (peak C) in the wash-out experiments, the observed loss (about 50%) of the RBC signal over the interbolus interval (Fig. 2b) indicates that the signal decay is dominated by T_1^*. The longer T_1^* of the putative pulmonary tissue signal (peak B) damps the amplitude of the periodic variation, and we merely see a period of accumulation (Fig. 2c).

The interpretation of the rather long T_1^* of 49.6 s for the putative combined signals from the plasma and adipose tissue (peak A) requires careful explication. We have observed that the T_1 in oxygenated human blood *in vitro* is 13.5 s, dropping to 4.2 s in human venous blood (*15*). This trend has been confirmed in another *in vitro* study using a different procedure (*16*). Given that the blood circulation time in the rat is only several seconds long (*17*), the deoxygenation that sets in, as the blood reaches the venous part of the circulation, should eradicate the plasma signal quickly. The short T_1 of ^{129}Xe in venous blood implies that recirculation of hyperpolarized ^{129}Xe is insignificant. The long T_1^* of peak A, therefore, compels us to postulate the existence of reservoirs, possibly adipose tissue, where ^{129}Xe becomes sequestered when arterial blood is rich in hyperpolarized ^{129}Xe, and enables the ^{129}Xe signal to be maintained.

Previously, an *in vivo* xenon signal in tissue, at about 199 ppm, with a T_1^* of about 20 seconds, was reported from a mouse (*4*). While consistent with our present results, the broad linewidth of the peak precluded assignments of tissue

resonances in that report. The long-lasting *in vivo* blood and tissue signals reported here advance the prospect of imaging with hyperpolarized ^{129}Xe. Furthermore, the spectral resolution achieved should permit acquisition of chemical shift-selected ^{129}Xe images of the gas space, blood vessels, and tissue. Figure 3a shows a sequential time series of six hyperpolarized ^{129}Xe images of the lung gas space from a living rat. Figure 3b shows the image sum of all six images of the series. The two lungs are clearly visible, and correspond to signal voids in the corresponding proton image (Fig. 3c). An important clinical use may be in the performance of both ventilation and perfusion imaging of patients with pulmonary pathology.

ACKNOWLEDGMENTS

This work was supported by the Uehara Memorial Foundation (K.S.); the Whitaker Foundation (M.S.A.); and the Air Force Office of Scientific Research, the George W. Burch Foundation, and the Smithsonian Institution (E.O., R.L.W.). We thank Daniel Kacher, Ching-Hua Tseng, and Glenn Wong for technical assistance, Drs. Daniel Williamson and Robert Mulkern for stimulating discussions, and K.S. thanks Drs. Yasushi Miyashita and Bruce Rosen for their encouragement.

REFERENCES

1. M. S. Albert, G. D. Cates, B. Driehuys, W. Happer, B. Saam, C. S. Springer Jr., and A. Wishnia, *Nature* 370, 199 (1994).
2. H. Middleton, R. D. Black, B. Saam, G. D. Cates, G. P. Cofer, R. Guenther, W. Happer, L. W. Hedlund, G. A. Johnson, K. Juvan, and J. Swartz, *Magn. Reson. Med.* 33, 271 (1995).
3. P. Weathersbee and L. Homer, *Undersea Biomed. Res.* 7, 277 (1980).
4. M. E. Wagshul, T. M. Button, H. F. Li, Z. Liang, and A. W. Wishnia, Abstracts of the Society of Magnetic Resonance, 3rd Annual Meeting, Nice, p. 1194, 1995.
5. K. Sakai, A. M. Bilek, C. H. Tseng, D. Balamore, R. L. Walsworth, E. Oteiza, F. A. Jolesz, and M. S. Albert, Abstracts of the Experimental Nuclear Magnetic Resonance Conference, 37th Annual Meeting, Pacific Grove, p. 323, 1996.
6. K. Sakai, A. M. Bilek, C. H. Tseng, D. Balamore, R. L. Walsworth, E. Oteiza, F. A. Jolesz, and M. S. Albert, Abstracts of the International Society for Magnetic Resonance, 4th Annual Meeting, New York, 1996, in press.
7. N. D. Bhaskar, W. Happer, and T. McClelland, *Phys. Rev. Lett.* 49, 25 (1982).
8. W. Happer, E. Miron, S. Schaefer, D. Schreiber, W. A. Van Wijngaarden, and X. Zeng, *Phys. Rev. A* 29, 3092 (1984).
9. D. Raftery, H. Long, T. Meersmann, P. J. Grandinetti, L. Reven, and A. Pines, *Phys. Rev. Lett.* 66, 584 (1991).
10. G. D. Cates, R. J. Fitzgerald, A. S. Barton, P. Bogorad, M. Gatzke, N. R. Newbury, and B. Saam, *Phys. Rev. A* 45, 4631 (1992).
11. U.S. Department of Health and Human Services, *in* ''Guide for the Care and Use of Laboratory Animals,'' NIH Publication 85-23, Washington, DC, 1985.
12. M. S. Albert, V. D. Schepkin, and T. F. Budinger, *J. Comp. Assist. Tomogr.* 19, 975 (1995).
13. R. F. Tilton, Jr., and I. D. Kuntz Jr. *Biochemistry* 21, 6850 (1982).
14. J. B. West, *in* ''Respiratory Physiology—The Essentials,'' 5th ed., Williams & Wilkins, Baltimore, 1995.
15. M. S. Albert, D. Balamore, K. Sakai, D. Kacher, R. L. Walsworth, E. Oteiza, and F. A. Jolesz, Abstracts of the International Society for Magnetic Resonance, 4th Annual Meeting, New York, 1996, in press.
16. S. Peled, C. H. Tseng, L. Nascimben, R. L. Walsworth, and F. A. Jolesz, Abstracts of the Experimental Nuclear Magnetic Resonance Conference, 37th Annual Meeting, Pacific Grove, p. 375, 1996.
17. C. L. Prosser and F. A. Brown Jr. *in* ''Comparative Animal Physiology,'' 2nd ed., Saunders, Philadelphia, 1961.